Food Chemistry: X 24 (2024) 101950

Contents lists available at ScienceDirect

Food Chemistry: X

journal homepage: www.sciencedirect.com/journal/food-chemistry-x

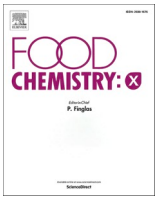

Development of a β-lactamase-based aggregation-induced emission lateral flow strip for the detection of clavulanic acid in Milk

Xiaonan Wang [a,1], Tong He [a,1], Leina Dou [a,b], Licai Ma [a], Xuezhi Yu [a], Zhanhui Wang [a], Kai Wen [a,*]

[a] National Key Laboratory of Veterinary Public Health Security, College of Veterinary Medicine, China Agricultural University, Beijing Key Laboratory of Detection Technology for Animal-Derived Food Safety, and Beijing Laboratory for Food Quality and Safety, Beijing 100193, PR China
[b] College of Veterinary Medicine, Northwest A&F University, Yangling 712100, Shaanxi, PR China

ARTICLE INFO

Keywords:
PC1 β-lactamases
Lateral flow strip
Rapid detection
Clavulanic acid;

ABSTRACT

Lack of biorecognition elements significantly hinders the development of rapid detection methods for clavulanic acid (CA). To address this, we expressed Class A β-lactamases PC1 in vitro and demonstrated its high affinity for CA. Then we investigated the recognition mechanisms of PC1 for CA and identified key contact amino acids: Ser70, Lys73, Ser130, Glu166, and Lys234. Furthermore, PC1 was utilized as a novel biorecognition element to establish a "pseudo-immuno" lateral flow strip (LFS) for CA detection. Aggregation-induced emission fluorescence microspheres (AIE@FM) and biotin-streptavidin (Bio-SA) were integrated to improve the detection performance of PC1-based LFS. Results showed that the sensitivity (cut-off value) of PC1-based AIE(Bio-SA)-LFS was enhanced 2-fold and 4-fold compared to basic AIE@FM-LFS and traditional Au-based LFS, respectively. Eventually, the proposed PC1-based AIE(Bio-SA)-LFS was successfully verified in milk samples with a cut-off value of 20 ng mL^{-1}. This study provides a powerful tool for on-site CA monitoring for the first time.

1. Introduction

Clavulanic acid (CA), a potent naturally occurring inhibitor of bacterial β-lactamases, is derived from the organism *Streptomyces clavuligerus* (Neu & Fu, 1978). It exhibits activity against a broad spectrum of both Gram-positive and Gram-negative bacteria (Saudagar, Survase, & Singhal, 2008). CA has been extensively included in the treatment with Amoxicillin (AX) to treat bovine mastitis (Peng et al., 2021). Excessive residues of CA in fresh milk not only triggers severe allergic reactions, itching, and difficulty breathing, but also enhance the risk of developing antibiotic resistance in humans to β-lactam antibiotics (Huttner et al., 2020; Mancabelli et al., 2021; Torres et al., 2016). Many regulatory agencies in various countries have set stringent CA standards in fresh milk used for consumption, for instance, the European Union (EU) and China have established the maximum residue limits (MRLs) of CA in milk as 200 μg/kg. Hence, there is an urgent demand to develop detection method for CA screening in fresh milk.

The detection of CA was previously relied on instrumental analysis, such as high-performance liquid chromatography (HPLC) (Guo, Chen, Yue, & Yu, 2017) and ultra performance liquid chromatography/tandem mass spectrometry (UPLC-MS/MS) assay (Liu et al., 2016). Often instrumental experimental steps are complex and require many specific pre-treatments for samples. However, the relatively time-consuming nature of these instrumental techniques is a shortcoming when prompt results are urgently needed. In marked contrast, antibody-based immunoassays are facile and do not require complicated equipment for operation, thus it has been widely employed for small-molecule detection in the fields of biomedicine, food safety, and environmental surveillance (Bai et al., 2021; Li et al., 2023; Wang et al., 2023). Unfortunately, the production of antibody against CA has proven remarkably difficult due to the absence of a characteristic spatial structure and the poor stability of CA both in vivo and in vitro (Barbero et al., 2019; Edwards, Dewdney, Dobrzanski, & Lee, 1988; Meng et al., 2016; Torres et al., 2016). Therefore, the pursuit of antibody substitutes or mimetics against CA has emerged as a viable approach.

So far, many natural macromolecular proteins (e.g. penicillin-binding proteins (PBP) (Lu et al., 2024), dihydropteroate synthase (DHPS) (He, Liu, & Wang, 2021; He, Liu, & Wang, 2022), tetracycline

* Corresponding author.
E-mail address: wenkai@cau.edu.cn (K. Wen).
[1] These authors contribute equally to this work

https://doi.org/10.1016/j.fochx.2024.101950
Received 27 September 2024; Received in revised form 29 October 2024; Accepted 30 October 2024
Available online 15 November 2024

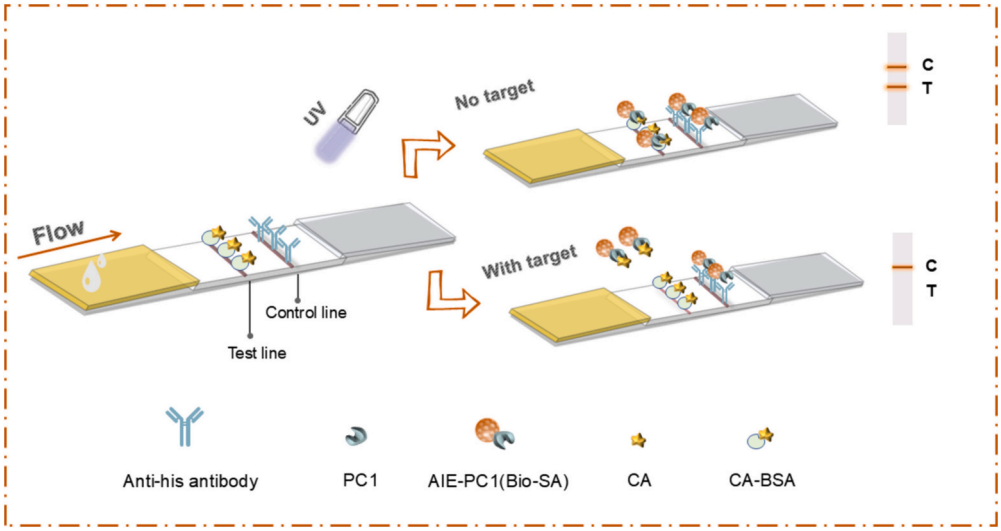

Scheme 1. Schematic of CA detected by PC1-based AIE-LFS(Bio-SA).

repressor (TetR)) (Li et al., 2023; Xia, Liu, & Wang, 2023) have been utilized as antibody substitutes or mimetics to establish "pseudo-immunoassays" (Chen et al., 2018; He et al., 2023). Inspired by the potent binding of CA to β-lactamases, it is theoretically plausible that β-lactamases could function as antibodies, thereby establishing a competitive detection method for CA. PC1 is a representative class A β-lactamase, an enzyme that confers resistance to β-lactam antibiotics by hydrolyzing their β-lactam ring (Bush, 2018; Tooke et al., 2019). The structure of PC1 comprises two distinct domains: a five-stranded antiparallel β-sheet domain and a fully α-helical domain. CA works by binding irreversibly to the active site of PC1, thereby inhibiting its activity and preventing the hydrolysis of the antibiotic (Brogden et al., 1981). Based on this principle, we propose utilizing the PC1 β-lactam to develop a "pseudo-immunoassay" for detecting clavulanic acid. To our knowledge, no attempts have been reported to establish a detection method that utilizes PC1.

A lateral flow strip (LFS) is widely employed to detect small molecule drug residues in food samples due to its simplicity, rapidity, and user-friendliness (Bai et al., 2022; Dou et al., 2022). Many conventional LFS employ colloidal gold particles as signal labels. Nonetheless, the low sensitivity of colloidal gold particles often fails to meet the demands for enhanced sensitivity applications (Liu et al., 2020). A wide variety of fluorescence microspheres has been incorporated into LFS to enhance detection capability (Wu et al., 2021; Zhou et al., 2022; Zou et al., 2022), but they suffer from aggregation-caused quenching (ACQ). To overcome the drawbacks associated with ACQ observed in conventional fluorochromes, aggregation-induced emission (AIE) dyes have emerged as an alternative approach (Dou, Li, Wang, Shen, & Yu, 2022; Li et al., 2020), offering enhanced sensitivity compared to colloidal gold particles.

In this work, PC1 was expressed in vitro and utilized as a recognition reagent to develop a "pseudo-immunoassay". The recognition mechanism was investigated through molecular docking. An AIE fluorescence microsphere (AIE@FM) labeled PC1 integrated with a biotin-streptavidin (Bio-SA) system was used to establish a lateral flow assay (LFS) method for the rapid detection of CA in milk (Scheme 1). Then, we evaluated the PC1-based AIE(Bio-SA)-LFS in terms of its quantitative standard curve, limit of detection (LOD), linear range (LR), specificity, repeatability, and recovery (RC). The proposed PC1-based AIE(Bio-SA)-LFS can be used as a sensitive, simple, rapid, and versatile method for the quantitative detection of CA in milk samples.

2. Materials and methods

2.1. Materials and apparatus

Sulbactam, and Clavulanic acid standard substances (solid, HPLC-grade, purity ≥99.0 %) were provided by Beijing WDWK Biotechnology Co., Ltd. (Beijing, China). 1-ethyl-3-(3-dimethylaminopropyl) carbodiimide hydrochloride (EDC), N-hydroxysuccinimide (NHS), Bovine serum albumin (BSA), and 2-(N-morpholino)-ethanesulfonic acid (MES) were sourced from Sigma-Aldrich, Inc. (St. Louis, USA). AIE@FM was purchased from AIE Institute (Guangdong, China). Streptavidin, Biotin, His tag antibody was obtained from Solarbio Science & Technology Co., Ltd. (Beijing, China). Nitrocellulose (NC) membranes, absorbent pads, glass fibers, and polyvinyl chloride (PVC) back plates provided from WDWK Biotechnology Co., Ltd. (Beijing, China). The Ultra-pure water was prepared by an ultrapure water system (Millipore Co., Ltd., USA). All remaining chemicals reagents were of analytical grade and derived from the Sinopharm Group Chemical Reagent Co., Ltd. (Shanghai, China).

2.2. Expression and purification PC1 β-lactamase

Amino acid sequences of PC1 β-lactamase were obtained from GenBank (Accession: TJX78208.1) (Huang, So, Chen, Leung, & Yao, 2020). Then, the gene sequence of PC1 β-lactamase was codon optimized for *E. coli* and synthesized by Genewiz Biotechnology Co., Ltd. (Nanjing, China). Subsequently, the target fragment was inserted into an express vector pET-28a, and the constructed recombinant plasmid was transformed into *E. coli* BL21 (DE3)-competent cells for expression. Single colonies were picked up and inoculated into LB medium containing 50 μg/mL kanamycin. Cells were grown at 37 °C until OD_{600} reached 0.8, then, 0.5 mM IPTG was added to induce expression of the recombinant protein. Cells were harvested by centrifugation for 15 min at 3200*g*. Then the cells were resuspended using PBS (containing 10 mM imidazole) and lysed by sonication for 15 min. The expressed PC1 β-lactamase was purified by Ni-NTA column purification system. Purified PC1 β-lactamase was further characterized by SDS-PAGE, Western blotting assay and circular dichroism (CD).

2.3. Surface Plasmon resonance (SPR) analysis

The binding affinity between PC1 and CA was evaluated using surface plasmon resonance (SPR) analysis, a critical validation step in the construction of the "PC1 based pseudo-immunoassay." The SPR analysis

was performed using a Biodot AD1520 array printer to print CA, diluted in DMSO, onto a photocrosslinkable sensor chip in quadruplicate. Rapamycin (positive control) and DMSO (negative control) were also printed on the chip. Following vacuum drying, the chip was subjected to UV irradiation for photocrosslinking. It was then sequentially washed with DMF, ethanol, and water, dried with nitrogen gas, and placed into the Berthold bScreen LB 991 microarray system for SPR analysis. PC1 was pre-incubated in 20 mM Tris-HCl (pH 8.0, containing 40 mM $MgCl_2$) and subsequently diluted in PBS to prepare test solutions at concentrations of 10, 40, 160, 640, 800, and 2560 nM. These solutions were injected into the Berthold bScreen LB 991 microarray system under the following conditions: flow rate of 0.5 μL/s, association time of 600 s, dissociation time of 360 s, and a temperature of 4 °C. The dissociation constant (KD), association rate constant (Ka), and dissociation rate constant (Kd) were then calculated by fitting the association and dissociation phases to a 1:1 Langmuir binding model.

2.4. Conjugation of AIE-PC1

The conjugation of AIE-SA: A 10 μL AIE@FM was mixed with 104 μL MES solution (50 mM, pH 6.0) and then the mixture was sonicated for 60 s. Then, 63 μL Sulfo-NHS (1 mM) and 63 μL EDC (1 mM) were added sequentially to the mixture. The tube containing mixture was placed on a plate shaker for 15 min at room temperature. After that, 0.1 % Tween-20 was added to the mixture and then centrifuged for 15 min (15,000 g). The obtained precipitate was resuspended in coupling buffer (borax/boric-acid solution, 40 mM, pH 8.0). 0.1 mg streptomycin was added to the coupling buffer containing AIE@FM and the mixture was incubated in a plate shaker for 1 h. Afterward, 0.1 % Tween-20 was added to the mixture, and then the mixture centrifuged, and discard the supernatant fraction. 50 mM ethanolamine (pH 7.4, containing 2 % BSA) was added to block the precipitate at room temperature for 1 h. After centrifugation, the sediment was resuspended in 400 μL Tris-HCl (0.1 M, pH 8.0). The obtained AIE-SA was stored at 4 °C for further use. The biotinylation of PC1 β-lactamase was conducted following the protocols outlined in

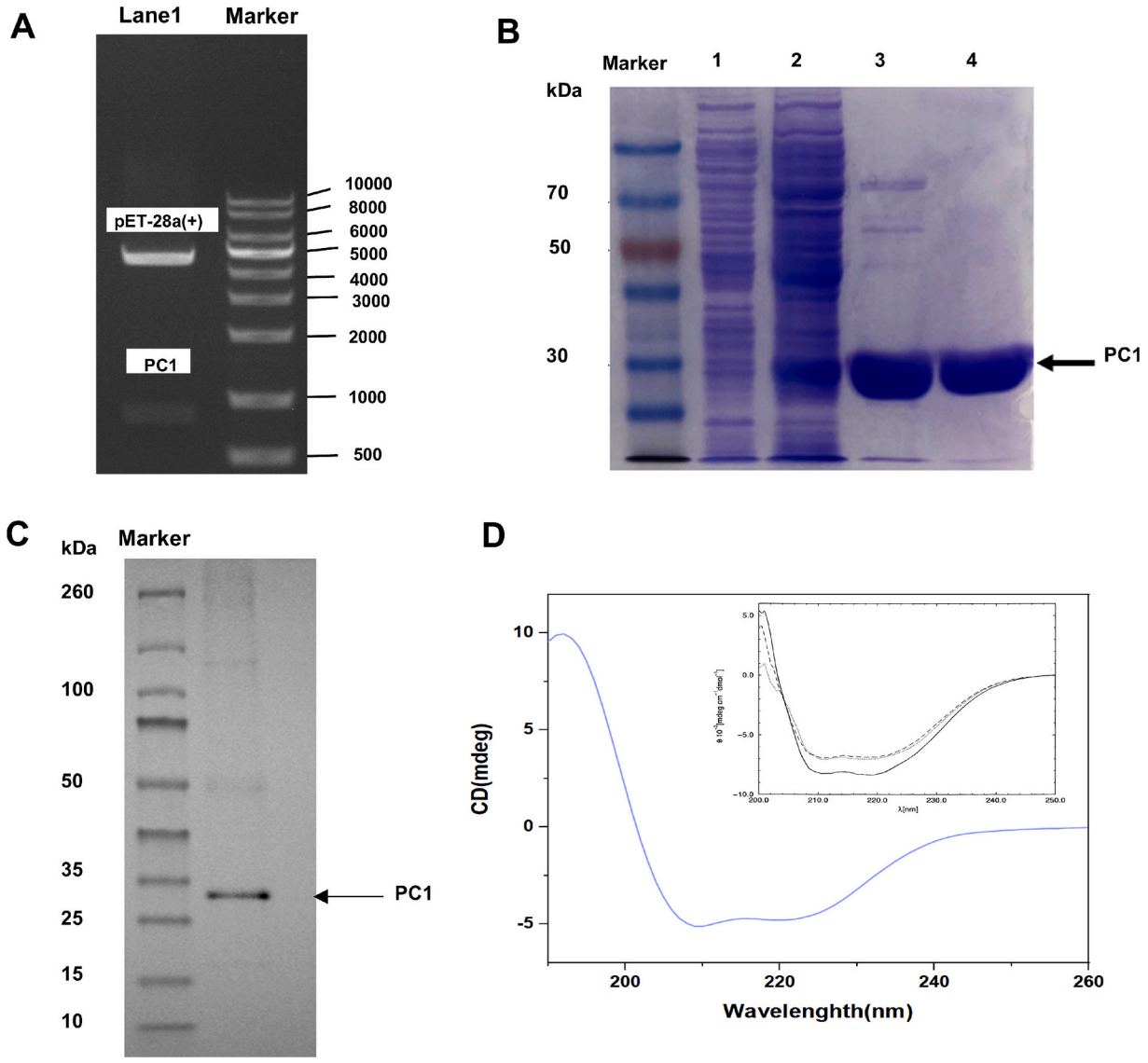

Fig. 1. Characterization of PC1 β-Lactamase (A) Agarose gel electrophoresis result of the express vector pET-28a(+)-PC1 (Lane 1). (B) SDS-PAGE results of the PC1 (lane 1, before IPGT induction; lane 2, after IPGT induction; lane 3, supernatant; lane 4, purified supernatant). (C) Western blotting result of the PC1. (D) Far-UV circular dichroism spectra of PC1 β-Lactamase (blue line) at 25 °C (the inset figure was the reported CD spectrum). The concentration of PC1 β-Lactamase was 0.5 mg/mL, and the solutions contained 0.1 M potassium phosphate at pH 7.4. (For interpretation of the references to color in this figure legend, the reader is referred to the web version of this article.)

the "Crosslinking Technical Handbook" provided by Thermo Fisher. Finally, the AIE-PC1 probe was obtained by incubating AIE-SA with biotinylated protein for two hours at room temperature. The obtained AIE-PC1 was characterized using UV–vis, dynamic light scattering (DLS) and zeta potential measurements (Zeta).

2.5. Synthesis of capture antigen (CA-BSA)

CA-BSA was synthesized according to literature (Wen et al., 2020). Briefly, 15 mg EDC and 25 mg NHS were added to 1 mM CA which was dissolved in 500 μL DMF. After stirring for 12 h, the activation was completed and the mixture was regarded as Solution I. Dissolve 0.001 mM BSA in 10 mL PBS completely, and then place it in the refrigerator at −20 °C for 2 min. After cooling, the mixture was regarded as Solution II. Take the solution I slowly added to the corresponding solution II, and the mixture was stirred for 24 h. The resultant solution further subjected to the dialysis, and the dialysis solution was changed every 12 h. After 72 h of dialysis, the captured antigen CA-BSA was obtained and subsequently measured using MALDI-TOF-MS. The coupling ratio of hapten to BSA was determined by the eq. (1):

$$\text{Coupling ratio} = \left(M_{conjugates} - M_{BSA}\right)/M_{haptens} \quad (1)$$

2.6. Development the PC1-based AIE(bio-SA)-LFS

As illustrated in Scheme 1, the PC1-based AIE(Bio-SA)-LFS was constructed by sequentially assembled nitrocellulose (NC) membrane, sample pad, absorbent pad, and PVC backing pad. The CA-BSA and anti-his tag antibody were dispensed on to the NC membrane to form Test line (T) and Control line (C), respectively. The prepared blocking buffer was used to treat the sample pad for 2 h, and then the sample pad was dried at 37 °C overnight. The absorbent pad and PVC backing pad were used without additional treatment. After systematically assembling all modules, ensuring an approximate 2 mm overlap between adjacent parts, the final product was cut into 3 mm sections and stored at 4 °C until needed.

Sensitivity is mainly influenced by the amount of CA-BSA and biotinylated PC1 β-lactamase in the competitive format. Thus, firstly, we need to optimize the molar ratios between AIE@FM-SA and biotinylated PC1 β-lactamase, different ratios (AIE@FM-SA: biotinylated PC1 β-lactamase = 10:1, 100:1, 1000:1, 10,000:1) were prepared and employed in LFS. The changes in fluorescence intensity and competitive inhibition ratio were quantified. Considering the inhibition ratio and the fluorescence intensity of the C line and T line, the appropriate ratio between AIE@FM-SA and biotinylated PC1 β-lactamase was selected for subsequent tests. Secondly, different concentration (4, 2, 1, 0.5, 0.25, and 0.125 mg/mL) of CA-BSA were diluted in 10 mM PBS and sprayed on the T line. Antigen concentration screening also involved assessing both the fluorescence strength of the C-line and T-line, as well as the inhibition ratio. Different buffers, including H_2O, phosphate buffer saline (PBS), britton-robinson buffer solution (BB), carbonate buffer solution (CB), and FL diluent (10 mM PBS, pH 8.0, containing 0.25 % BSA, 0.5 % Tween-20, and 1 % sucrose) were prepared by our laboratory. Lastly, appropriate reaction time (1, 5, 10, 15 min) also evaluated to enhance sensitivity.

2.7. Analytical performance of LFS based on AIE@FM and colloidal gold particles in PBS

The CA standard was spiked into PBS (0.01 M, pH 7.4) at a final concentration of 0, 2.5, 5, 10, 20, 40, and 80 ng mL^{-1}. A total of 200 μL of the spiked solution was added into a low-attachment tube, followed by the addition of either 5 μL the probe. After incubating for 3 min, the test strip was placed into the mixture for 10–15 min. Subsequently, the test strips were read, and the resulting data were collected. A calibration curve was generated by plotting T line fluorescence intensity as the Y-axis and CA concentration as the X-axis. The standard curve was constructed using the Y-axis values and the logarithmic transformation of the X-axis values, and a linear regression equation was derived for quantitative analysis.

2.8. Application of PC1-based AIE(bio-SA)-LFS for CA assay in real samples

Analysis in real samples was conducted by adding known concentrations of CA standards into blank samples. The CA-free raw milk samples were provided by WDWK Biotechnology Co., Ltd., and the raw milk was pretreated through simple dilution (5-fold). The specificity of PC1-based AIE(Bio-SA)-LFS was evaluated by detecting other chemical analogues, including sulbactam, amoxicillin, and norfloxacin at a concentration of 100 ng mL^{-1}.

2.9. Molecular docking

The obtained PC1 gene was translated into an amino acid sequence using DNAman software, and homology modeling was conducted utilizing the obtained sequence. The 100 % homologous model (PDB ID: 3BLM) was used for molecular docking by using Discovery Studio. Firstly, the PC1 model was docked with CA to locate the binding pocket for this study, then several important parameters were determined (including key contact amino acids and specific binding sites).

3. Results and discussion

3.1. Characterization of the PC1

As shown in Fig. 1A, the expression vector yields both parts of the vector (5369 bp) and the genes of the PC1 (843 bp) after enzyme digestion, demonstrating that the construction of the recombinant plasmid was successful. The PC1 β-Lactamase consists of 281 amino acids, with a calculated molecular mass of 31,350 Da. As illustrated in Fig. 1B, SDS-PAGE analysis revealed that the target protein predominantly exists in a soluble formation, with an observed molecular weight of approximately 30 kDa, aligning with theoretical predictions. Additionally, the target protein incorporates a His tag, enables its detection through a Western blotting (WB) assay utilizing an anti-His tag antibody. As shown in Fig. 1C, the WB experiment demonstrated that the desired PC1 β-Lactamase was obtained. Subsequently, the Circular dichroism (CD) in the far UV range (190–260 nm) was employed to provide whether the secondary structure of PC1 changed upon expression and purification. As shown in Fig. 1D, by CD, the purified PC1 β-Lactamase exhibited a similar amount of secondary structure to that reported previously (Pieper, Hayakawa, Li, & Herzberg, 1997). After performing a series of structural characterizations on the expressed PC1, its binding capacity to CA was confirmed through SPR assay (**Fig. S1**). The equilibrium dissociation constant (KD) of PC1 binding to CA was calculated to be $9.72*10^{-9}$ M (Ka = $2.75*10^{4}$, Kd = $2.68*10^{-4}$, KD=Kd/Ka). The KD is inversely related to affinity, indicating that a lower KD value (corresponding to a lower concentration) signifies a higher affinity of the recognition element for the target. High affinity antibodies are typically regarded as being in the low nanomolar range (10^{-9} M), while those with very high affinity are in the picomolar range (10^{-12} M) (Patten et al., 1996). SPR analysis results show that PC1 exhibits high affinity levels for CA, comparable to high affinity antibodies, making it suitable for the development of "pseudo-immunoassay." These results altogether revealed that the desired PC1 β-Lactamase was obtained, so it can be used for the following experiments.

3.2. Characterization of CA-BSA

The hapten CA was covalently coupled to BSA using the active ester method to produce hapten-protein conjugates (CA-BSA), which served

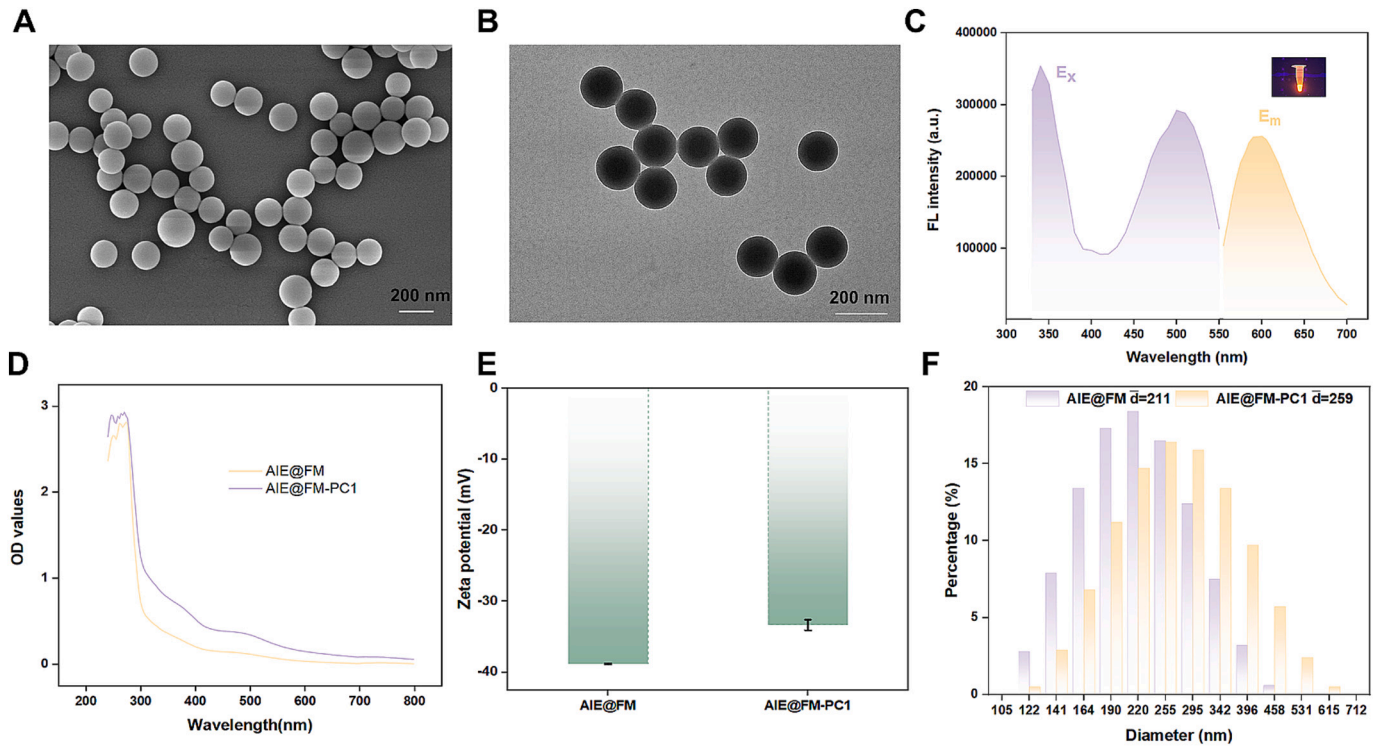

Fig. 2. Characterization of the AIE@FM and synthesized AIE@FM-PC1. SEM of the diluted AIE@FM (A), TEM of the AIE@FM (B), Fluorescence excitation spectrum (E_x) and emission spectrum (E_m) of AIE@FM. The inserted image shows the fluorescence color of AIE@FM (C). UV–vis absorption spectra of the AIE@FM and AIE@FM-PC1 (D), Zeta potential values of AIE@FM and AIE@FM-PC1 (E); Particle size percentage of AIE@FM and AIE@FM-PC1 (F);

as "antigens," and were subsequently analyzed by MALDI-TOF-MS (**Fig. S2**). A shift in molecular weight was observed when compared to the carrier protein (BSA), indicating successful coupling of the CA to BSA. The approximately 10:1 coupling ratio of CA to BSA was determined by the eq. (1) in the 2.5 section.

3.3. Principle of PC1 based AIE(bio-SA)-LFS

$$E + I \rightleftharpoons E{\cdot}I \rightarrow (E - I)$$

(E is the PC 1 β-lactamase and I is the β-lactamase inhibitor CA. E·I, reversible complex; E-I, stable acyl enzyme)

As previously shown, the general reaction mechanism between β-lactamase and β-lactamase inhibitors involves the initial formation of a reversible complex, **E·I**, between PC 1 β-lactamase and the inhibitor CA. Subsequently, this complex may proceed to a stabilized acyl enzyme **E-I** due to the reaction of the inhibitor with a serine residue in the enzyme's active site. Our PC1-based AIE(Bio-SA)-LFS is based on the indirect competitive mode between PC1 and irreversible β-lactamase inhibitor CA. Dyes inherent with AIE features are utilized to fabricate AIE fluorescence microspheres (AIE@FM) for the purpose of enhancing detection performance. To enhance the sensitivity of the LFS, we further introduced the streptavidin-biotin signal amplification system alongside AIE@FM, as we all know, the interaction between streptavidin and its ligand biotin is the strongest receptor-ligand interaction. Such a Bio-SA system has been effectively utilized in the development of methods for amplifying the signal, thereby expanding the sensitivity range for the target. The PC1 β-lactamase was labeled with AIE@FM through streptavidin-biotin system functions as a sensitive fluorescence reporter (AIE-PC1). T-line was immobilized with CA-BSA, wherein CA-BSA was intended to competitively with free CA to bind to the labeled PC1 β-lactamase. Mixed solution containing the AIE-PC1 probe can flow in the direction of the absorbent pad due to capillary force. For CA-free samples, the AIE-PC1 probes migrate along the NC membrane until they bound by immobilized CA-BSA. Unbounded AIE-PC1 probe continues to migrate and is subsequently captured by the anti-His antibody immobilized on control line. Hence, two fluorescent bands are visible on the test strip when illuminated with UV light, and quantification of fluorescent signal intensities was conducted using a portable immunofluorescence reader. In the presence of CA, the AIE-PC1 probe bind with CA first in the sample and limited β-lactamase's binding sites was occupied. Thus, CA-BSA on the T line cannot capture the AIE-PC1 probe, only control line was detectable with the naked eye under UV light. In light of this rationale, the T line fluorescence intensity decreases gradually with the increase in CA concentration, and the obvious changes in intensity can be easily seen by naked eyes.

3.4. Characterization of AIE@FM and AIE-PC1

The aggregation-caused quenching ACQ phenomenon was first reported by Förster and Kasper (1954) and refers to the intense intermolecular π − π stacking interactions experienced by adjoining luminophores, which result in the quenching of their emission (Bakalova et al., 2006; Förster & Kasper, 1954; Zhelev, Ohba, & Bakalova, 2006). To overcome the issue, aggregation-induced emission (AIE) agents have emerged and provided new choices for fluorescence sensing (Mei, Leung, Kwok, Lam, & Tang, 2015). In this study, various characterization techniques were employed to validate the AIE@FM, including SEM, TEM, UV–Vis spectroscopy, and fluorescence spectroscopy. Micrographs obtained by SEM (Fig. 2A) and TEM (Fig. 2B) revealed that the AIE@FM were homogeneous spherical, with a consistent diameter averaging approximately 190 nm. In general, larger particle sizes result in greater surface areas, allowing for more amount of PC1 to be coupled. Previous literature also indicated that FM with particle sizes of 200 nm or 300 nm are typically chosen for use in small molecule competition methods (Li et al., 2015; Li et al., 2019). Therefore, the particle size of AIE@FM was appropriate for the construction of the LFS. As depicted in Fig. 2C, the left pale purple curve represents the excitation spectra of AIE@FM,

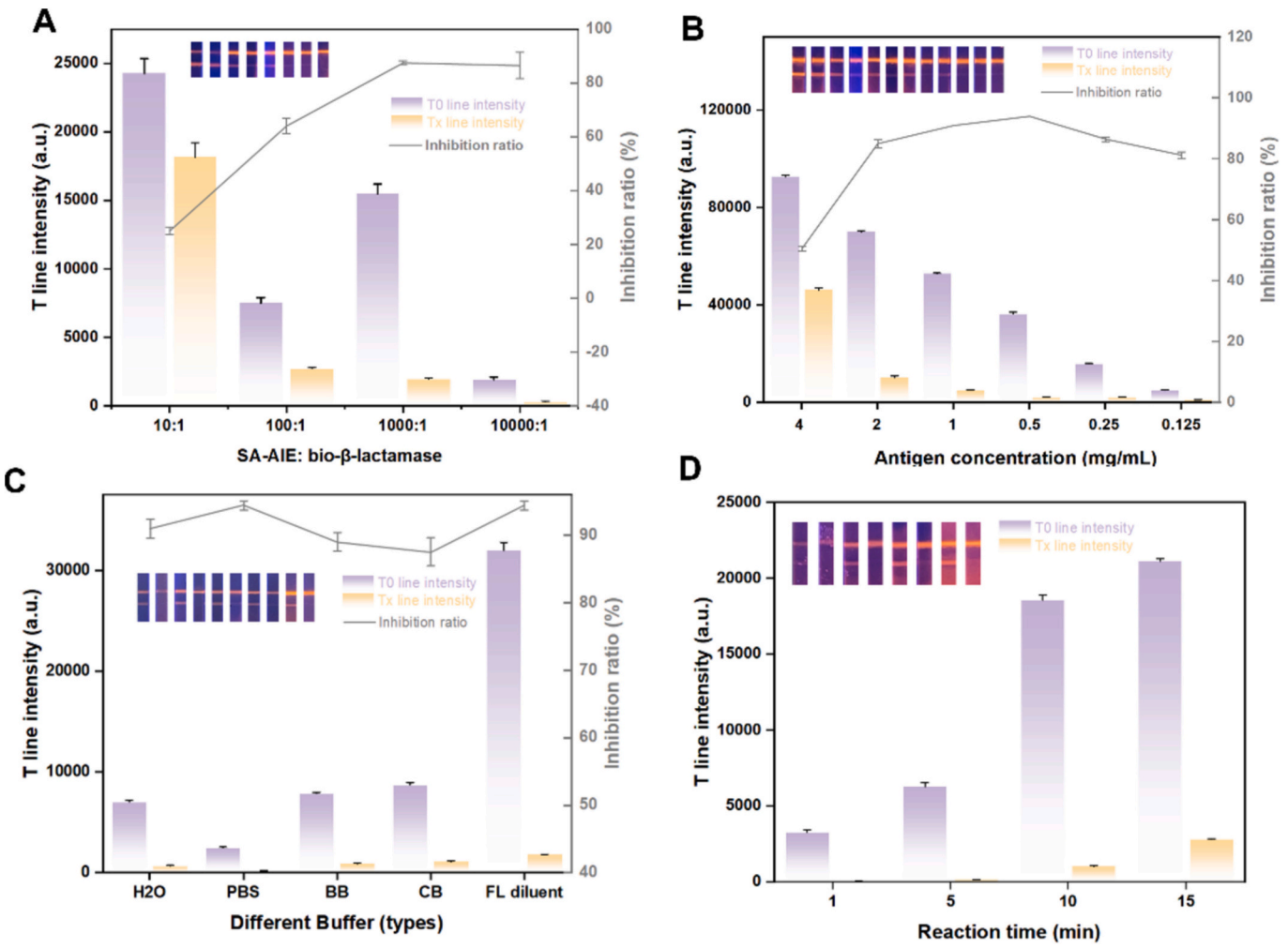

Fig. 3. Optimization results of the PC1-based AIE(Bio-SA)-LFS. Ratios between biotinylated PC1 β-lactamase and AIE@FM-SA (A). Concentration of "antigen" (B). Different buffer types (C)and reaction time for the proposed LFS.

while the right yellow curve represents the emission spectra of AIE@FM. The AIE@FM exhibited red fluorescence with an emission peak at 610 nm, which provides higher sensitivity and lower background signals, making them highly suitable for fluorescence-based detection applications. To verify the PC1 successful conjugates to the AIE@FM by Bio-SA system, UV–vis spectra, Zeta potential, and size distribution were performed. It can be seen that the positions of the absorption peaks of the AIE@FM did not change before or after PC1 labeling, which indicates that the basic structure of the AIE@FM is not affected by PC1 labeling (Fig. 2D). Zeta potential analysis indicated a surface potential of −38.3 mV for AIE@FM and − 33.3 mV for AIE-PC1. The change in zeta potential upon PC1 labeling demonstrated that PC1 was successfully conjugated to the surface of AIE@FM (Fig. 2E). As shown in Fig. 2F, the increased particle size distribution of AIE-PC1, further verifying the successful synthesis of AIE-PC1. This condition arose because the protein conjugated to AIE@FM altered the refractive index (Hu et al., 2023). Additionally, the AIE-PC1 remained well-dispersed.

3.5. Optimization of analytical parameters

Given the fluorescence signal derived from the specific PC1-CA identify binding, crucial parameters including the ratios between biotinylated PC1 and AIE@FM-SA, "antigen" concentration, reaction buffer types, and reaction time were investigated. Typically, the results of analytical factors, where T0 stands for the fluorescence signal intensity of T line without analytes, Tx stands for the corresponding intensity at analyte with a concentration of 20 ng mL^{-1} for CA, respectively. The evaluation criteria are founded on the signal intensity, inhibition ratio (1-signal intensity (Tx)/ signal intensity (T0) *100 %, a higher value of inhibition ratio indicated better inhibition effect), and the signal intensity of T line should be strong enough to meet the requirements of visual inspection in the field. The ratio of biotinylated PC1 and AIE@FM-SA was an important initial factor as the amount of PC1 directly influences signal intensity. As shown in Fig. 3A, excess amount of PC1 could cause a decreased inhibition ratio and a low sensitivity, which was unfavorable for the screening. Considering factors of T line signal intensity and inhibition ratio, 1000:1 was chosen as the optimal ratio between AIE@FM-SA and biotinylated PC1. The "antigen" (CA-BSA) concentration on the T line influenced the capture ability of the AIE@ PC1 probe. T0 intensity increased with the increased CA-BSA concentration, and the inhibition ratio decreased when the CA-BSA concentration was over 0.5 mg/mL (Fig. 3B). Therefore, 0.5 mg/mL was used as the optimal CA-BSA concentration of AIE@PC1-LFS. A suitable buffer would favor the binding of PC1 with CA and resulting in higher sensitivity. As illustrated in Fig. 3C, compared with the different buffer types, the signal intensity and inhibition ratio achieved the highest value when the buffer was FL diluent. Finally, as seen from Fig. 3D, the signal intensity was increased following increased reaction time and the signal intensity reached plateau when reaction time was 10 min. Thus, 10 min was chosen in this study. The detection performance of the PC1-based AIE(Bio-SA)-LFS, AIE@FM-LFS, and colloidal gold particles was compared. For the AIE@FM-LFS, and colloidal gold

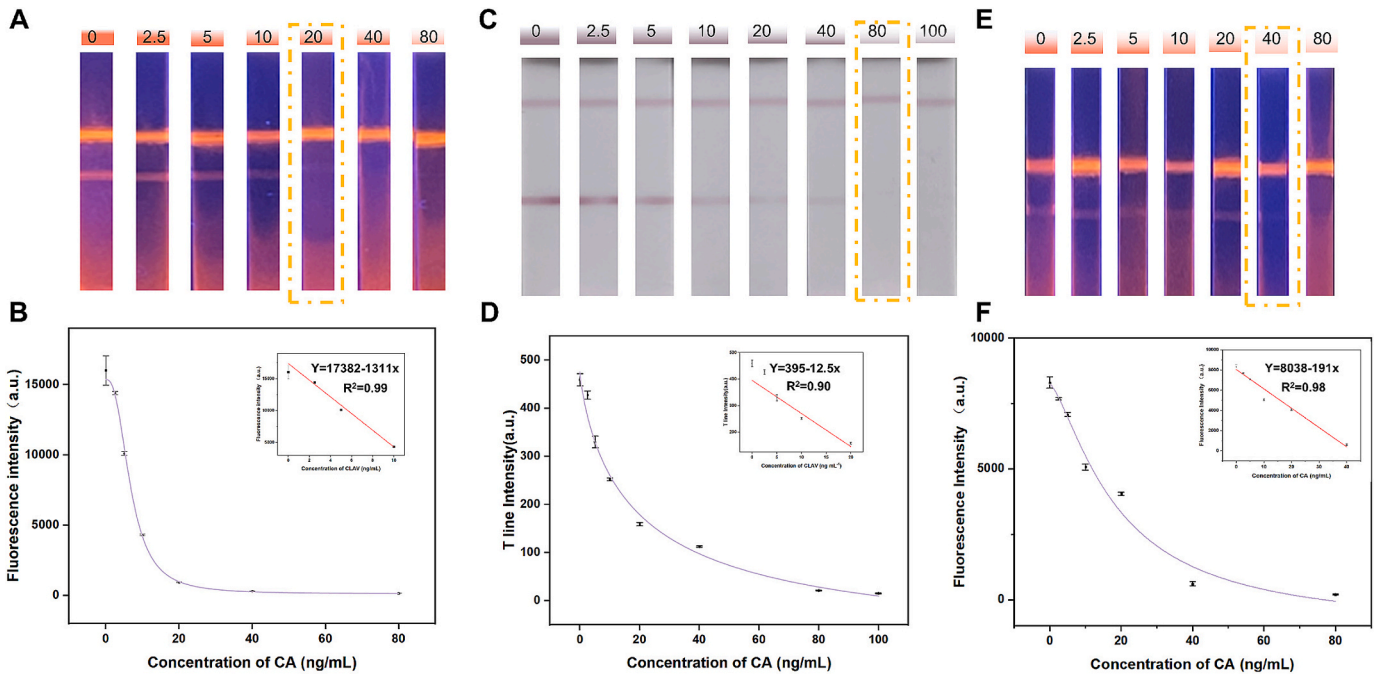

Fig. 4. Fig. 4: Analysis performances of the three patterns based LFSs: (A). Analysis performances of the PC1-based AIE(Bio-SA)-LFS and correspondingly regression equation and linear relationship (B). Analysis performances of PC1-based AIE@FM-LFS without SA-bio system (C) and correspondingly regression equation and linear relationship (D). Analysis performances of the PC1-based Au-LFS (E) and correspondingly regression equation and linear relationship (F).

particles (Au) based LFS, a variety of experimental conditions such as concentration of PC1 β-lactamase, buffer types and reaction time are depicted in **Fig.S3** and **S4**. In addition, the experimental conditions, including the composition of the blocking buffer, the rate of dispensing, and the concentrations of anti-His antibody (C line) for the manufactured LFS, are listed in **Table S1**.

3.6. Methods performance

The detection capabilities of PC1-based LFS utilizing AIE@FM, both with and without the Bio-SA system, as well as with Au Labels, were evaluated in terms of sensitivity and linear range. Sensitivity and linear range of PC1-based AIE(Bio-SA)-LFS were determined by standard spiked recovery experiments using various CA concentrations, as they are crucial evaluation criteria for assessing the performance of PC1-based AIE(Bio-SA)-LFS detection. Here, the cut-off value (COV) was introduced for the semi-quantitative detection of CA, where COV was recognized as the minimum CA concentration that makes T line invisible. Traditional PC1-based Au-LFS and PC1-based AIE@FM-LFS without Bio-SA system were also measured. As depicted in Fig. 4A, B and C, the fluorescence or color intensity of the T-line exhibited a gradual decrease concurrent with increasing CA concentration, consistent with findings from prior studies. The results (Fig. 4A, C and E**)** revealed that the COVs of PC1-based LFS for CA detection using the AIE@FM labels integrated Bio-SA system, AIE@FM and the conventional Au label were 20, 40, and 80 ng mL^{-1}, which suggested 2-fold and 4-fold enhancements compared with AIE@FM-LFS and traditional Au-based LFS, respectively. The observed increase in sensitivity could be primarily attributed to the signal amplification of AIE@FM replacing Au, which highlights the superiority of AIE@FM in LFS for CA detection. Additionally, the contribution of streptavidin-biotin signal amplification strategy in PC1-based AIE(Bio-SA)-LFS deserved a brief discussion owing to the high affinity of streptavidin-biotin binding (each streptavidin can bind four biotin molecules). Leveraging its unique binding advantage, Bio-SA has previously been used as a “cross-linker” to efficiently couple biorecognition elements to signal labels (Sun, Zhang, Zhao, Xia, & Liu, 2020; You, Lim, & Gunasekaran, 2020). Moreover, Lakshmipriya et al. utilized streptavidin-conjugated Au nanoparticles to enhance the detection of clotting protein factor IX (FIX), achieving a low limit of detection (LOD) of 100 pM (Lakshmipriya et al., 2013). Thus, higher coupling efficiency in the proposed Bio-SA assisted AIE-PC1 probe significantly enhanced the utilization efficiency of PC1, which contributed to improved sensitivity in competitive-type LFS. Furthermore, the regression equations and linear relationship of the PC1-based AIE(Bio-SA)-LFS, PC1-based AIE@FM-LFS, and PC1-based Au-LFS were fitted before applying the proposed LFS in real sample. In Fig. 4B, the regression equation of PC1-based AIE(Bio-SA)-LFS (y (a.u.) =103.05+ 15,254.95/(1 + (x/6.78)2.59), $R^2 = 0.99$) was obtained for the dynamic range from 0 to 20 ng mL^{-1}. Additionally, a linear relationship was observed for concentrations ranging from 0 to 10 ng mL^{-1}, expressed as y (a.u.) = −1311[CA] + 17,382, with an R^2 value of 0.99 (Fig. 4c inset). For the conventional PC1-based Au-LFS, the regression equation was obtained and the linear relationship could be fitted as y (a. u.) = −12.5 [CA] +395 ($R^2 = 0.90$, Fig. 4D) within the concentration range of 0 to 20 ng mL^{-1}. For the PC1-based AIE@FM-LFS, the regression equation was obtained and the linear relationship could be fitted as y (a. u.) = −191[CA] +8038 ($R^2 = 0.98$, Fig. 4E) within the concentration range of 0 to 40 ng mL^{-1}. In the above linear equations, where y represented the fluorescence signal intensity of the T-line measured by Reader software, [CA] represented the concentration of the target analyte. Collectively, these results validated the efficacy of incorporating the Bio-SA signal amplification strategy into the PC1-based AIE@FM-LFS system.

3.7. Analysis in actual samples

To simulate the complicated sample matrix, several of potential interfering structural analogues including sulbactam, amoxicillin, and norfloxacin (chemical structures were given in **Fig. S5**) were chosen to assess the specificity of proposed method. As shown in **Fig. S6,** T line intensity displayed significant decrease toward CA (100 ng mL^{-1}), while neither these potential interfering structural analogues cannot cause obvious changes. Simultaneously, the coexistence of structural analogues and target analytes were tested and similar T line intensity were observed. Specificity results indicated the the satisfactory selectivity and

Table 1
Comparison with previous methods for CA detection.

Method	sample	Target	LOD (ng mL^{-1})	Detection range	Sample pretreatment	References
HPLC	milk	CA	140	–	Acetonitrile dried with nitrogen gas	Guo et al.
UPLC-MS/MS	milk	CA	20	20–1000	Acetonitrile dried with nitrogen gas	Liu et al.
LFS	milk	CA	20 (cut-off)	0–20	Dilution	This work

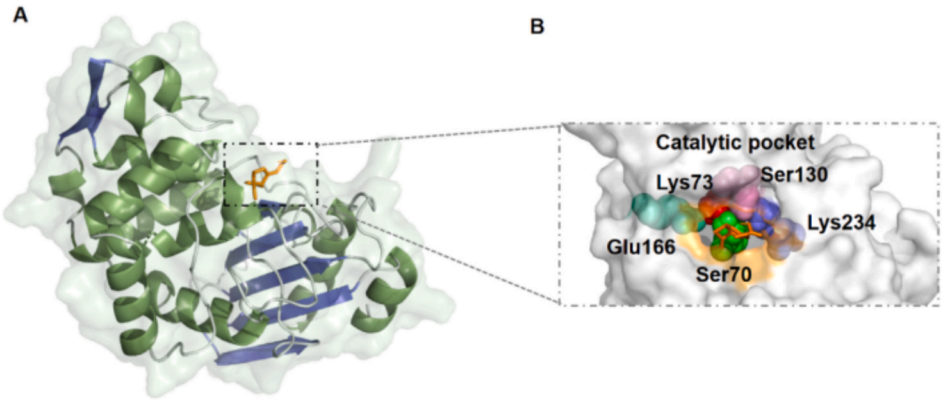

Fig. 5. Close observation of the docking complex with CA: (1) PC1/CA (orange), (B) Catalytic pocket: Lys represented in green, Lys 73 represented in red, Ser130 represented in pale-purple, Glu represented in pale-cyan, and Lys 234 represented in mazarine. Pale-orange represents residues within the range of ligand 5 A. (For interpretation of the references to color in this figure legend, the reader is referred to the web version of this article.)

robust ability to resist potential coexisting structural analogue interferences in CA sensing. After performing specificity of PC1-based AIE (Bio-SA)-LFS toward CA sensing, the actual milk sample was employed to verify the screening capability of the proposed method. Known concentrations of CA (0–80 ng mL^{-1}) were spiked in milk. After sample pretreatment, the acquired sample solution was measured using the PC1-based AIE(Bio-SA)-LFS. As showed in **Fig. S7**, the FL intensity of T line decrease gradually with the raising of CA concentration. **Fig. S7** demonstrated the COV in actual sample was 20 ng mL^{-1}, which was well consistent with anticipate results. Furthermore, standard spiked method was used to assess the accuracy and reliability of PC1-based AIE(Bio-SA)-LFS in actual milk sample through recovery experiments. The average recoveries of the PC1-based AIE(Bio-SA)-LFS ranged from 78.5 % to 83 % with RSD values (4.2 %–8.6 %) lower than 15 % (**Table S2**), indicates that the PC1-based AIE(Bio-SA)-LFS method demonstrates satisfactory accuracy and high reliability for detecting CA in milk samples.

3.8. Comparison with previous methods for CA detection

This study developed a lateral flow strip for CV detection based on PC1 β-lactamase for the first time. The assays that have been reported for CA detection in milk were summarized in Table 1. For comparison with the present method, some essential parameters of those methods were collected. First, the PC1 based AIE(Bio-SA)-LFS developed in this study exhibits high sensitivity, with a cut-off value that rivals UPLC-MS/MS but is relatively lower than HPLC. Second, the milk sample pretreatment was simple and fast, diluting is all that is needed for testing. Third, the designed sensor strip here is applicable for visual colorimetric detection with the aid of a handheld UV lamp, making it suitable for outdoor applications. Overall, the present PC1-based AIE(Bio-SA)-LFS showed generally better performance than the previously reported assays.

3.9. Intermolecular interaction of PC1 and CA

The crystal structure of PC1 has been elucidated; however, the crystal structure of the PC1/CA complex has not yet been determined. To further understand the binding mode and binding sites between CA and PC1, we constructed a PC1 model using homology modeling and simulated the final docking conformation of PC1 and CA (the lowest energy conformation) through molecular docking. PyMOL software was used to analyze and visualize the docking results. The molecular docking results revealed that the active pocket of PC1 presents a groove-like shape, with the β-lactam moiety of the CA molecule penetrating into the groove (Fig. 5A and B). The nucleophilic amino acid Ser70, located at the junction of the β-sheet domain and the α-helical domains, acts as the catalytic site. Additionally, Ser70 interacts with another conserved seryl residue, Ser130, which is positioned between the two functionally important lysine residues, Lys73 and Lys234. Overall, most of the key catalytic residues are situated within 5 Å of the CA ligand, including Ser70 (green), Lys73 (red), Ser130 (pale-purple), Glu166 (pale-cyan), and Lys234 (mazarine). These amino acids form an active pocket during the catalytic process, consistent with previous reports (Pieper et al., 1997). As previously reported, the opening of the β-lactam ring does not lead to substantial alterations in the relative positions of the atoms involved in class A β-lactamases-substrate binding (Herzberg & Moult, 1987; Moews, Knox, Dideberg, Charlier, & Frère, 1990; Strynadka et al., 1992). Hence, while the conformation of the complex formed by the β-lactam ring-opened CA molecule and PC1 is not provided in this study, it can be inferred that the PC1/CA complex is not likely to differ significantly between the states before and after the opening of the β-lactam ring of CA. Though the molecular docking applied in the current work could not fully characterize these interactions, they provide a more intuitive and convenient approach compared to crystallography.

4. Conclusion

Lateral Flow Strips (LFS) are commonly used for screening small molecule drug residues in foodstuff sample, and the choice of recognition elements and signal systems is crucial for determining their sensitivity and specificity. Due to the lack of distinctive spatial structure and the poor stability of CA, the production of anti-CA antibodies is notoriously challenging, which impedes the development of antibody-based

immunoassays for CA detection. In this study, we used natural PC1 β-lactamase as the recognition element for the first time and constructed a "pseudo-immuno" LFS for detecting CA. Molecular docking confirmed the binding conformation of PC1 and CA. Additionally, AIE@FM-based fluorescent signaling and the SA-biotin system were introduced to enhance the performance of the CA-LFS. Results demonstrated that the proposed PC1-based AIE(Bio-SA)-LFS exhibited a 4-fold increase in sensitivity compared to traditional Au labels CA-LFS. This method could be used for screening CA residues in large-scale milk samples. Furthermore, this approach provides a new and promising strategy for enhancing sensitivity, particularly for target analytes of interest where antibody production is challenging.

CRediT authorship contribution statement

Xiaonan Wang: Writing – original draft, Resources, Methodology, Formal analysis, Conceptualization. **Tong He:** Methodology, Investigation, Formal analysis, Data curation, Conceptualization. **Leina Dou:** Visualization, Validation, Investigation, Formal analysis. **Licai Ma:** Methodology, Investigation. **Xuezhi Yu:** Validation, Resources, Methodology. **Zhanhui Wang:** Supervision, Resources, Project administration. **Kai Wen:** Writing – review & editing, Validation, Supervision, Conceptualization.

Declaration of competing interest

The authors declare that they have no known competing financial interests or personal relationships that could have appeared to influence the work reported in this paper.

Acknowledgments

The authors would like to thank the financial support of "Fourteen Five-Year" program funds (National Key Research and Development Program of China, Grant 2022YFF1101000).

Appendix A. Supplementary data

Supplementary data to this article can be found online at https://doi.org/10.1016/j.fochx.2024.101950.

Data availability

No data was used for the research described in the article.

References

Bai, F., Bu, T., Li, R., Zhao, S., He, K., Li, M., … Wang, L. (2022). Rose petals-like bi semimetal embedded on the zeolitic imidazolate frameworks based-immunochromatographic strip to sensitively detect acetamiprid. *Journal of Hazardous Materials, 423*(Pt B), Article 127202. https://doi.org/10.1016/j.jhazmat.2021.127202

Bai, Y., Jiang, H., Zhang, Y., Dou, L., Liu, M., Yu, W., Wen, K., Shen, J., Ke, Y., Yu, X., & Wang, Z. (2021). Hydrophobic moiety of capsaicinoids haptens enhancing antibody performance in immunoassay: Evidence from computational chemistry and molecular recognition. *Journal of Agricultural and Food Chemistry, 69*(34), 9957–9967. https://doi.org/10.1021/acs.jafc.1c03657

Bakalova, R., Zhelev, Z., Aoki, I., Ohba, H., Imai, Y., & Kanno, I. (2006). Silica-shelled single quantum dot micelles as imaging probes with dual or multimodality. *Analytical Chemistry, 78*(16), 5925–5932. https://doi.org/10.1021/ac060412b

Barbero, N., Fernández-Santamaría, R., Mayorga, C., Martin-Serrano, Á., Salas, M., Bogas, G., … Torres, M. J. (2019). Identification of an antigenic determinant of clavulanic acid responsible for IgE-mediated reactions. *Allergy, 74*(8), 1490–1501. https://doi.org/10.1111/all.13761

Brogden, R. N., Carmine, A., Heel, R. C., Morley, P. A., Speight, T. M., & Avery, G. S. (1981). Amoxycillin/clavulanic acid: A review of its antibacterial activity, pharmacokinetics and therapeutic use. *Drugs, 22*(5), 337–362. https://doi.org/10.2165/00003495-198122050-00001

Bush, K. (2018). Past and present perspectives on β-lactamases. *Antimicrobial Agents and Chemotherapy, 62*(10). https://doi.org/10.1128/AAC.01076-18

Chen, C., Luo, J., Li, C., Ma, M., Yu, W., Shen, J., & Wang, Z. (2018). Molecularly imprinted polymer as an antibody substitution in pseudo-immunoassays for chemical contaminants in food and environmental samples. *Journal of Agricultural and Food Chemistry, 66*(11), 2561–2571. https://doi.org/10.1021/acs.jafc.7b05577

Dou, L., Bai, Y., Liu, M., Shao, S., Yang, H., Yu, X., … Yu, W. (2022). "Three-to-one" multi-functional nanocomposite-based lateral flow immunoassay for label-free and dual-readout detection of pathogenic bacteria. *Biosensors & Bioelectronics, 204*(114093), Article 114093. https://doi.org/10.1016/j.bios.2022.114093

Dou, L., Li, Q., Wang, Z., Shen, J., & Yu, W. (2022). AIEgens: Next generation signaling source for immunoassays? *ACS Sensors, 7*(11), 3243–3257. https://doi.org/10.1021/acssensors.2c02165

Edwards, R. G., Dewdney, J. M., Dobrzanski, R. J., & Lee, D. (1988). Immunogenicity and allergenicity studies on two beta-lactam structures, a clavam, clavulanic acid, and a carbapenem: Structure-activity relationships. *International Archives of Allergy and Applied Immunology, 85*(2), 184–189. https://doi.org/10.1159/000234500

Förster, T., & Kasper, K. (1954). Ein konzentrationsumschlag der fluoreszenz. *Zeitschrift Für Physikalische Chemie (Frankfurt Am Main, Germany), 1*(5_6), 275–277. https://doi.org/10.1524/zpch.1954.1.5_6.275

Guo, P., Chen, Y., Yue, C., & Yu, G. (2017). Simultaneous determination of clavulanic acid and tazobactam in bovine milk by HPLC. *Food Additives & Contaminants:Part A, 34*(4), 617–623. https://doi.org/10.1080/19440049.2016.1277271

He, T., Cui, P. L., Zhang, S., Fan, Y. H., Jin, Q. S., & Wang, J. P. (2023). Development of a receptor based signal amplified fluorescence polarization assay for multi-detection of 35 sulfonamides in pork. *Food Chemistry: X, 19*(100867), Article 100867. https://doi.org/10.1016/j.fochx.2023.100867

He, T., Liu, J., & Wang, J. P. (2021). Development of a dihydropteroate synthase-based fluorescence polarization assay for detection of sulfonamides and studying its recognition mechanism. *Journal of Agricultural and Food Chemistry, 69*(46), 13953–13963. https://doi.org/10.1021/acs.jafc.1c05674

He, T., Liu, J., & Wang, J. P. (2022). Evolution of a natural dihydropteroate synthase and development of a signal amplified fluorescence method for detection of 44 sulfonamides in milk. *Analytica Chimica Acta, 1234*(340481), Article 340481. https://doi.org/10.1016/j.aca.2022.340481

Herzberg, O., & Moult, J. (1987). Bacterial resistance to β-lactam antibiotics: Crystal structure of β-lactamase from *staphylococcus aureus* PC1 at 2.5 Å resolution. *Science, 236*(4802), 694–701. https://doi.org/10.1126/science.3107125

Hu, L., Chen, Z., Li, T., Ye, X., Luo, Q., & Lai, W. (2023). Comparison of oriented and non-oriented antibody conjugation with AIE fluorescence microsphere for the immunochromatographic detection of enrofloxacin. *Food Chemistry, 429*(136816), Article 136816. https://doi.org/10.1016/j.foodchem.2023.136816

Huang, L., So, P.-K., Chen, Y. W., Leung, Y.-C., & Yao, Z.-P. (2020). Conformational dynamics of the helix 10 region as an allosteric site in class a β-lactamase inhibitory binding. *Journal of the American Chemical Society, 142*(32), 13756–13767. https://doi.org/10.1021/jacs.0c04088

Huttner, A., Bielicki, J., Clements, M. N., Frimodt-Møller, N., Muller, A. E., Paccaud, J.-P., & Mouton, J. W. (2020). Oral amoxicillin and amoxicillin-clavulanic acid: Properties, indications and usage. *Clinical Microbiology and Infection, 26*(7), 871–879. https://doi.org/10.1016/j.cmi.2019.11.028

Lakshmipriya, T., Fujimaki, M., Gopinath, S. C. B., Awazu, K., Horiguchi, Y., & Nagasaki, Y. (2013). A high-performance waveguide-mode biosensor for detection of factor IX using PEG-based blocking agents to suppress non-specific binding and improve sensitivity. *The Analyst, 138*(10), 2863–2870. https://doi.org/10.1039/c3an00298e

Li, P., Bai, Y., Jiang, H., Zhang, Y., Li, Y., Duan, C., Wen, K., Yu, X., & Wang, Z. (2023). Broad-specificity antibody profiled by hapten prediction and its application in immunoassay for fipronil and major metabolites. *Journal of Hazardous Materials, 441*(129931), Article 129931. https://doi.org/10.1016/j.jhazmat.2022.129931

Li, S., Chen, D., Liu, Z., Tao, S., Zhang, T., Chen, Y., Bao, L., Ma, J., Huang, Y., Xu, S., Wu, L., & Chen, S. (2023). Directed evolution of TetR for constructing sensitive and broad-spectrum tetracycline antibiotics whole-cell biosensor. *Journal of Hazardous Materials, 460*(132311), Article 132311. https://doi.org/10.1016/j.jhazmat.2023.132311

Li, X., Shen, J., Wang, Q., Gao, S., Pei, X., Jiang, H., & Wen, K. (2015). Multi-residue fluorescent microspheres immunochromatographic assay for simultaneous determination of macrolides in raw milk. *Analytical and Bioanalytical Chemistry, 407*(30), 9125–9133. https://doi.org/10.1007/s00216-015-9078-3

Li, X., Wu, X., Wang, J., Hua, Q., Wu, J., Shen, X., … Lei, H. (2019). Three lateral flow immunochromatographic assays based on different nanoparticle probes for on-site detection of tylosin and tilmicosin in milk and pork. *Sensors and actuators. B. Chemical, 301*(127059), Article 127059. https://doi.org/10.1016/j.snb.2019.127059

Li, Y., Liu, S., Ni, H., Zhang, H., Zhang, H., Chuah, C., … Tang, B. Z. (2020). ACQ-to-AIE transformation: Tuning molecular packing by regioisomerization for two-photon NIR bioimaging. *Angewandte Chemie, 59*(31), 12822–12826. https://doi.org/10.1002/anie.202005785

Liu, S., Dou, L., Yao, X., Zhang, W., Zhao, B., Wang, Z., Ji, Y., Sun, J., Xu, B., Zhang, D., & Wang, J. (2020). Polydopamine nanospheres as high-affinity signal tag towards lateral flow immunoassay for sensitive furazolidone detection. *Food Chemistry, 315*(126310), Article 126310. https://doi.org/10.1016/j.foodchem.2020.126310

Liu, Y., Zhu, K., Wang, J., Huang, X., Wang, G., Li, C., … Ding, S. (2016). Simultaneous detection and comparative pharmacokinetics of amoxicillin, clavulanic acid and prednisolone in cows' milk by UPLC-MS/MS. *Journal of Chromatography B, 1008*, 74–80. https://doi.org/10.1016/j.jchromb.2015.11.031

Lu, Z., Wang, X., Ma, L., Dou, L., Zhao, X., Tao, J., … Wen, K. (2024). Carba PBP: A novel penicillin-binding protein-based lateral flow assay for rapid phenotypic detection of carbapenemase-producing *Enterobacterales*. *Journal of Clinical Microbiology, 62*(2), Article e0012023. https://doi.org/10.1128/jcm.00120-23

Mancabelli, L., Mancino, W., Lugli, G. A., Argentini, C., Longhi, G., Milani, C., … Turroni, F. (2021). Amoxicillin-clavulanic acid resistance in the genus Bifidobacterium. *Applied and Environmental Microbiology, 87*(7). https://doi.org/10.1128/AEM.03137-20

Mei, J., Leung, N. L. C., Kwok, R. T. K., Lam, J. W. Y., & Tang, B. Z. (2015). Aggregation-induced emission: Together we shine, united we soar! *Chemical Reviews, 115*(21), 11718–11940. https://doi.org/10.1021/acs.chemrev.5b00263

Meng, X., Earnshaw, C. J., Tailor, A., Jenkins, R. E., Waddington, J. C., Whitaker, P., … Park, B. K. (2016). Amoxicillin and clavulanate form chemically and immunologically distinct multiple haptenic structures in patients. *Chemical Research in Toxicology, 29*(10), 1762–1772. https://doi.org/10.1021/acs.chemrestox.6b00253

Moews, P. C., Knox, J. R., Dideberg, O., Charlier, P., & Frère, J. M. (1990). β-Lactamase of bacillus licheniformis 749/C at 2 Å resolution. *Proteins, 7*(2), 156–171. https://doi.org/10.1002/prot.340070205

Neu, H. C., & Fu, K. P. (1978). Clavulanic acid, a novel inhibitor of β-lactamases. *Antimicrobial Agents and Chemotherapy, 14*(5), 650–655. https://doi.org/10.1128/aac.14.5.650

Patten, P. A., Gray, N. S., Yang, P. L., Marks, C. B., Wedemayer, G. J., Boniface, J. J., … Schultz, P. G. (1996). The immunological evolution of catalysis. *Science, 271*(5252), 1086–1091. https://doi.org/10.1126/science.271.5252.1086

Peng, M., Han, R., Guo, Y., Zheng, Y., Yang, F., Xu, X., & Hu, F. (2021). In vitro Combined Inhibitory Activities of β-Lactam Antibiotics and Clavulanic Acid Against bla KPC-2-Positive Klebsiella pneumoniae. *Infection and Drug Resistance, 14*, 361–368. https://doi.org/10.2147/IDR.S292612

Pieper, U., Hayakawa, K., Li, Z., & Herzberg, O. (1997). Circularly permuted beta-lactamase from *Staphylococcus aureus* PC1. *Biochemistry, 36*(29), 8767–8774. https://doi.org/10.1021/bi9705117

Saudagar, P. S., Survase, S. A., & Singhal, R. S. (2008). Clavulanic acid: a review. *Biotechnology Advances, 26*(4), 335–351. https://doi.org/10.1016/j.biotechadv.2008.03.002

Strynadka, N. C., Adachi, H., Jensen, S. E., Johns, K., Sielecki, A., Betzel, C., … James, M. N. (1992). Molecular structure of the acyl-enzyme intermediate in β-lactam hydrolysis at 1.7 Å resolution. *Nature, 359*(6397), 700–705. https://doi.org/10.1038/359700a0

Sun, T., Zhang, Y., Zhao, F., Xia, N., & Liu, L. (2020). Self-assembled biotin-phenylalanine nanoparticles for the signal amplification of surface plasmon resonance biosensors. *Mikrochimica Acta, 187*(8), 473. https://doi.org/10.1007/s00604-020-04461-x

Tooke, C. L., Hinchliffe, P., Bragginton, E. C., Colenso, C. K., Hirvonen, V. H. A., Takebayashi, Y., & Spencer, J. (2019). β-Lactamases and β-lactamase inhibitors in the 21st century. *Journal of Molecular Biology, 431*(18), 3472–3500. https://doi.org/10.1016/j.jmb.2019.04.002

Torres, M. J., Montañez, M. I., Ariza, A., Salas, M., Fernandez, T. D., Barbero, N., … Blanca, M. (2016). The role of IgE recognition in allergic reactions to amoxicillin and clavulanic acid. *Clinical and Experimental Allergy, 46*(2), 264–274. https://doi.org/10.1111/cea.12689

Wang, X., Lu, Q., Dou, L., Liu, M., Li, P., Yu, W., Yu, X., Wang, Z., & Wen, K. (2023). Broad-specificity indirect competitive enzyme-linked immunosorbent assay for aristolochic acids: Computer-aided hapten design and molecular mechanism of antibody recognition. *The Science of the Total Environment, 859*(Pt 1), Article 159941. https://doi.org/10.1016/j.scitotenv.2022.159941

Wen, K., Bai, Y., Wei, Y., Li, C., Shen, J., & Wang, Z. (2020). Influence of small molecular property on antibody response. *Journal of Agricultural and Food Chemistry, 68*(39), 10944–10950. https://doi.org/10.1021/acs.jafc.0c04333

Wu, Q., Yao, L., Qin, P., Xu, J., Sun, X., Yao, B., Ren, F., & Chen, W. (2021). Time-resolved fluorescent lateral flow strip for easy and rapid quality control of edible oil. *Food Chemistry, 357*(129739), Article 129739. https://doi.org/10.1016/j.foodchem.2021.129739

Xia, W. Q., Liu, J., & Wang, J. P. (2023). Evolution of a natural TetR protein and development of a Fe_3O_4 assisted semi-homogeneous fluorescent method for determination of tetracyclines in milk. *Analytica Chimica Acta, 1276*(341609), Article 341609. https://doi.org/10.1016/j.aca.2023.341609

You, Y., Lim, S., & Gunasekaran, S. (2020). Streptavidin-coated au nanoparticles coupled with biotinylated antibody-based bifunctional linkers as plasmon-enhanced immunobiosensors. *ACS Applied Nano Materials, 3*(2), 1900–1909. https://doi.org/10.1021/acsanm.9b02461

Zhelev, Z., Ohba, H., & Bakalova, R. (2006). Single quantum dot-micelles coated with silica shell as potentially non-cytotoxic fluorescent cell tracers. *Journal of the American Chemical Society, 128*(19), 6324–6325. https://doi.org/10.1021/ja061137d

Zhou, S., Xu, X., Wang, L., Liu, L., Kuang, H., & Xu, C. (2022). Rapid, on-site quantitative determination of higenamine in functional food using a time-resolved fluorescence microsphere test strip. *Food Chemistry, 387*(132859), Article 132859. https://doi.org/10.1016/j.foodchem.2022.132859

Zou, R., Guo, Y., Chen, Y., Zhao, Y., Zhao, L., Zhu, G., Liu, Y., Peters, J., & Guo, Y. (2022). Computer-aided profiling of a unique broad-specific antibody and its application to an ultrasensitive fluoroimmunoassay for five N-methyl carbamate pesticides. *Journal of Hazardous Materials, 426*(127845), Article 127845. https://doi.org/10.1016/j.jhazmat.2021.127845